NANO LETTERS

pubs.acs.org/NanoLett Letter

Achieving Ideal Magnetic Light Emission with Electric-Type Emitters

Ruizhao Yao, Hiroshi Sugimoto, Tianhua Feng, Minoru Fujii, Shimei Liu, Xinming Li, Sheng Lan, and Guang-Can Li*

Cite This: *Nano Lett.* 2024, 24, 13315−13323 Read Online

ACCESS | Metrics & More | Article Recommendations | Supporting Information

ABSTRACT: Optical magnetic dipole (MD) emission predominantly relies on emitters with significant MD transitions, which, however, rarely exist in nature. Here, we propose a strategy to transform electric dipole (ED) emission to a magnetic one by elegantly coupling an ED emitter to a silicon nanoparticle exhibiting a strong MD resonance. This emission mode transformation enables an artificially ideal magnetic dipole source with an MD purity factor of up to 99%. The far-field emission patterns of such artificial MD sources were experimentally measured, which unambiguously resolved their magnetic-type emission origin. This study opens the path to achieving ideal magnetic dipole emission with nonmagnetic emitters, largely extending the availability of magnetic light emitters conventionally limited by nature. Beyond the fundamental significance in science, we anticipate that this study will also facilitate the development of magnetic optical nanosource and enable potential photonic applications relying on magnetic light emission.

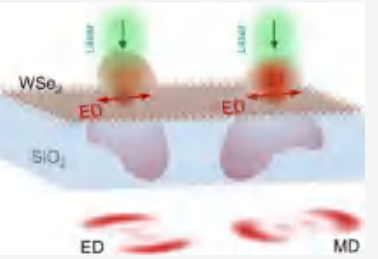

KEYWORDS: *ideal magnetic light emission, magnetic dipole resonances, silicon nanoparticles, in-plane dipoles, transition metal dichalcogenides*

Achieving strong magnetic light emission promises novel photonic applications such as active Huygens metasurfaces,[1,2] dynamic structural color display[3,4] and optical phased radars.[5,6] However, light emission of natural emitters originates mainly from their electric dipole (ED) transitions with the magnetic dipole (MD) transitions neglected. So far, prominent optical magnetic dipole emission had been observed only in few natural materials, say, rare-earth ions[7−9] and semiconductor quantum dots.[10] Moreover, the naturally occurring MD emission is usually dressed by significant ED characters because of contributions from concurrent ED transitions (Hereafter, we term emitters with simultaneous ED and MD transitions EMD emitters).[11] Effective suppression of residual ED transitions in such EMD emitters could be achieved by cryogenically cooling the emitters[12,13] or exploiting quantum emitters having larger spectral separation between ED and MD transitions, which, however, are either technically demanding or unavailable.

A promising strategy to realize a high-purity magnetic dipole source is exploiting metamaterials exhibiting resonant MD responses,[14] namely, metal-based split-ring resonators (SSRs),[15,16] ring-shaped nanoparticle oligomers,[17−19] and high-index dielectric nanostructures.[20,21] Rational design of the coupling between EMD emitters and these magnetic nanostructures allows significant modification of their emission properties via so-called magnetic Purcell effect,[22] typically manifested as accelerated or suppressed emission decay rates[23] and particularly, modulated spectral features and spatial profiles.[24,25] To exclusively enhance the MD emission from EMD emitters, it requires the emitters precisely located at the magnetic field hot spots of a nanostructure.[26] For magnetic plasmonic nanostructures, the associated magnetic field hot spots reside outside the constituent materials and thereby are accessible to external EMD emitters for strong magnetic-type coupling interactions.[27−29] Nevertheless, plasmonic nanoantenna coupled emitters suffer from significant emission quenching due to metal dissipation.[30,31]

Alternative solutions resort to high-index dielectric nanoantennas, benefiting from their low optical losses and strong Mie-type MD resonances.[32] However, the magnetic mode fields of simple dielectric nanostructures (nanoparticles, nanodisks, etc.) are deeply confined inside the constituent materials, inaccessible to external emitters.[26,33,34] Regarding this, recent studies proposed and demonstrated hollow silicon nanoparticles with magnetic field hot spots exposed to air.[35] Theoretical investigations predicted dramatically suppressed ED transitions of dipole emitters inside the open holes and thereby enhanced high-purity MD emission.[36−39] Despite these, precisely loading emitters into the nanoscale hollow regions remains challenging. The configuration of optical magnetic emitters placed closely near a dielectric nanoantenna has been employed to explore the magnetic Purcell effect.[40−42] While this out-of-cavity coupling marginally boosted the MD transition processes, it also induced equally intense ED

Received: August 5, 2024
Revised: October 3, 2024
Accepted: October 4, 2024
Published: October 9, 2024

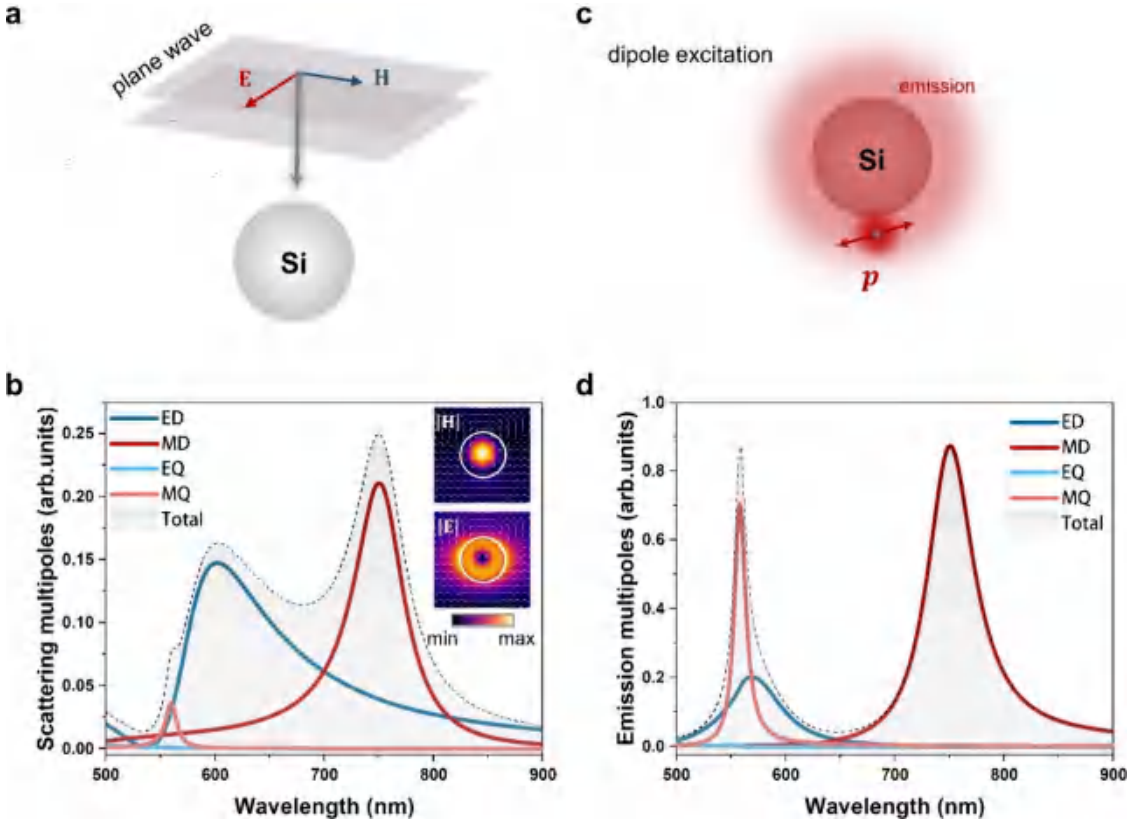

Figure 1. Mie resonances of a silicon nanosphere (SiNS) resolved under plane wave and electric dipole (ED) excitations. (a) Schematic illustration of the SiNS under plane wave excitation, with *E* and *H* indicating the electric and magnetic field components of the incident light, respectively. (b) Scattering cross sections and the multipolar contributions from the ED, magnetic dipole (MD), electric quadrupole (ED), and magnetic quadrupole (MQ) resonances under plane wave excitation, calculated for a SiNS with a diameter of 190 nm. Insets show the electric and magnetic near-field distributions at the MD resonance wavelength. (c) Schematic illustration of the electric dipole excitation (labeled as *p*) of a SiNS with the same diameter as in part (a). The dipole-SiNS distance is 1 nm. (d) Eemission multipoles calculated for the coupling structure in c.

emission from the coupled EMD emitters, largely due to the non-negligible coupling between excited ED transitions and the electric-type nanoantenna modes.

Instead of using MD emitters, in this article, we propose to realize high-purity MD emission based on emitters with pure ED transitions. This can be achieved by resonantly coupling ED emitters to a high-index dielectric nanoresonator exhibiting strong Mie-type MD resonances. Although a similar strategy has been well established in the communication frequency range to realize magnetic-type microwave radiation, its extension to optical frequencies for achieving ideal magnetic light emission is still missing. The implementation of this strategy at optical frequencies requires an optimized coupling configuration, in which electric emitters are preferentially oriented with respect to the MD mode fields of the resonator so they can exclusively couple to the structural MD mode. Such orientation control at the nanoscale is not readily available with typical optical emitters (molecules, quantum dots, etc.) having randomly oriented dipole moments. Here, we designed and fabricated such an optimized coupling structure by single silicon nanoparticles sitting on a transition metal dichalcogenides (TMDCs) monolayer. The emission of the TMDCs monolayer is dominated by in-plane oriented exciton dipoles which exclusively excite the MD-type antenna resonances of adjacent silicon nanoparticles and simultaneously suppress the residual ED-type antenna modes. This channels the local ED emission from the TMDCs into the radiative magnetic antenna mode and renders the antenna-coupled ED emitters as an ideal MD light source. Combining numerical simulations and experimental verifications, we demonstrated this design mechanism by a hybrid nanostructure comprised of a monolayered tungsten diselenide (WSe_2) coupled to a silicon nanoparticle, from which high-purity MD emission with a MD-purity-factor up to 99% was successfully resolved.

To illustrate how the silicon nanoparticles transform an ED emitter to an MD emitter, we start by discussing the fundamental resonances of a Si nanoparticle. It is well-known that a silicon nanoparticle with appropriate size supports multiple resonant Mie-type resonances within the visible range, which can be resolved from its scattering responses under plane wave illumination (see Figure 1a, b). Among them, the most pronounced one at the far right of the spectrum is the magnetic dipole resonance. Resonant excitation of this mode induces strong magnetic field localization at the nanoparticle center and simultaneously intense electric field confinement near the particle surfaces (the ring-shaped region, inset in Figure 1a). This implies the MD resonance can be efficiently excited by either a MD emitter located at the particle center (see Figure S1) or an ED emitter closely near the particle surface. We consider only the latter case, as the magnetic field "hot spot" deeply inside the particle is inaccessible to external MD emitters.

Prior to the experiment, we performed electromagnetic numerical simulations based on the finite element method (implemented with the commercial Comsol Multiphysics

https://doi.org/10.1021/acs.nanolett.4c03760
Nano Lett. 2024, 24, 13315−13323

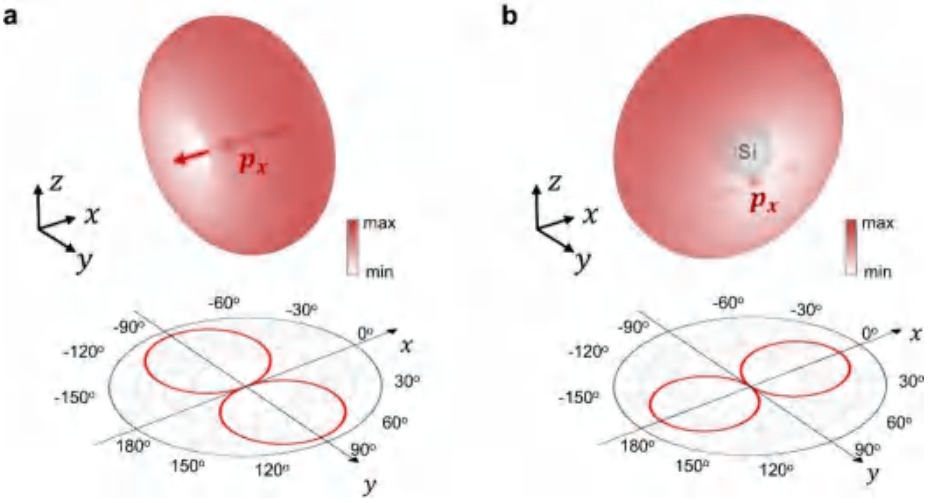

Figure 2. Modification of the emission pattern of an electric dipole source by a silicon nanoparticle. (a) Simulated emission pattern of an electric dipole in free space. The bottom panel shows the *xoy* plane cut through the source. (b) The emission pattern of the same ED source in (a) but with the presence of a silicon nanosphere. The emission wavelength is set at the magnetic dipole resonance of the particle.

package) to evaluate how a Si nanoparticle modifies the emission response of a nearby ED emitter. As depicted in Figure 1c, a point ED emitter was mimicked by an ED dipole placed 1 nm away from the surface of a silicon nanosphere (SiNS). Here we only consider the dipole orientation tangential to the particle surface, as the electric dipole oriented normal to the particle surface will invoke unwanted electric antenna mode (see Figure S2). Figure 1d shows the simulated emission spectrum of an electric dipole coupled to a SiNS (termed EDcSiNS thereafter), from which we can see that the SiNS-modified ED emission was dominated by a strong MD resonance at 750 nm, accompanied by a weaker peak at shorter wavelength. Multipolar decomposition of the total emission responses was performed (see Methods) and reveals that the weaker peak arises from the mixing of an ED and magnetic quadrupole (MQ) resonance. Particularly, compared to the scattering response of a SiNS illuminated by a plane wave (Figure 1b), the contribution of the electric mode component at the MD resonance wavelength is significantly suppressed in the emission response, thus leading to a high-purity MD emission mode. We define a mode-purity-factor (MPF) δ to quantitatively evaluate this effect, written as

$$\delta_{md} = \frac{P_{md}}{P_{total}} = \frac{P_{md}}{P_{md} + P_{ed} + P_{mq} + P_{eq} + \ldots} \approx \frac{P_{md}}{P_{md} + P_{ed} + P_{mq} + P_{eq}} \quad (1)$$

where δ_{md} is the mode-purity-factor of the MD resonance. P_{md}, P_{ed}, P_{mq} and P_{eq} denote the emission powers of the MD, ED, MQ and electric quadrupole (EQ) modes, respectively, all decomposed from the total emission power by performing a multipole expansion of P_{total}. By cutting off the expansion of P_{total} to these four lowest-order multipoles, we get a δ_{md} as high as 0.99. In a similar way, the MPF of the scattering MD resonance can be evaluated by replacing the emission powers of individual multipoles in eq 1 with their scattering cross sections calculated under plane wave excitation (Figure 1b). The corresponding results show an MPF of $\delta_{md}^{'} \sim 0.7$ for the scattering MD resonance, which indicates considerable contribution from other multipoles, mainly the ED mode ($\delta_{ed}^{'} \sim 0.3$). Further calculations show such significant mode mixing in a plane-wave illuminated SiNS can be resolved from its far-field scattering patterns (see Figure S3). Actually, the plane wave illumination can be seen as an extreme case of dipole excitation for which the dipole is placed at infinity. This can be rigorously derived from a theoretical model describing the scattering by a local electric dipole (see Section 4 in the Supporting Information),[43] which predicts a $\delta_{md} > 0.99$ for a dipole placed less than 10 nm away from the SiNS surface (Figure S4). With the theoretical mode, we can further understand and validate the simulation results.

Besides, the proximity of an ED emitter to a SiNS could significantly modify its emission pattern in the far field domain. We calculated the emission pattern of an ED emitter with and without coupling to a Si nanosphere. As shown in Figure 2a, the ED emitter in free space exhibits the well-known doughnut-shaped emission pattern, with the radiation dark axis, that indicates the direction along which the emission intensity is zero, aligned along the dipole orientation (p_x). In contrast, the EDcSiNS also exhibits a perfectly doughnut-shaped emission pattern at the MD resonance of the SiNS, but with a dark axis exactly orthogonal to the dipole orientation (Figure 2b). In other words, the presence of the SiNS rotates the emission pattern of an ED emitter by a degree of 90°. In theory, such an emission pattern is associated with an ED or MD source aligned along the *y* axis. Considering the extremely high δ_{md} at the MD resonance (Figure 1b), we can faithfully assign the rotated emission pattern to an MD source origin. This suggests in experiment we can verify the EDcSiNS enabled ED-MD transformation by comparing the emission patterns of a free ED emitter and one coupled to a SiNS.

In the experiment, fabrication of an EDcSiNS structure requires a substrate to support it. However, the presence of the substrate could significantly modify the emission patterns of emitters near it. Here we consider the configuration of an ED emitter positioned near a silica substrate with and without the presence of a SiNS. Our calculations show the affect of the silica substrate on the spectral characters of the nanoparticle and EDcSiNS resonances is negligible (Figure S5). The magnetic or electric nature of the light emission from these substrate-supported emitters can be resolved by inspecting

https://doi.org/10.1021/acs.nanolett.4c03760
Nano Lett. 2024, 24, 13315−13323

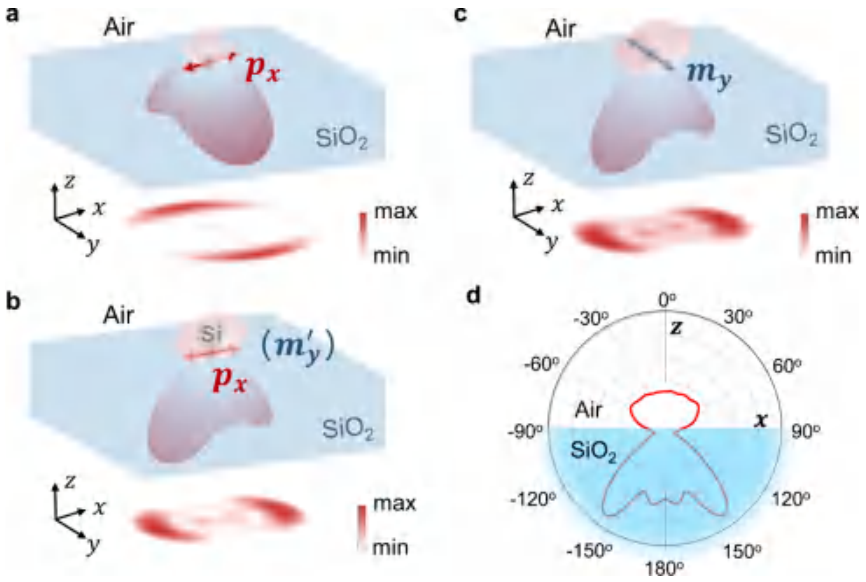

Figure 3. Emission patterns of dipole sources above a dielectric substrate. (a, b) Simulated emission patterns of a silica-supported electric dipole with the absence (a) and presence (b) of a silicon nanoparticle. m_y' denotes the magnetic dipole source formed from the coupling between an electric dipole (p_x) and a silicon nanoparticle. The dipole-substrate distance is 1 nm, and the nanoparticle is 1 nm above the dipole. The bottom insets show the far-field projections of the emission patterns. (c) Emission pattern of a bare magnetic dipole source (m_y) placed at the height of the nanoparticle center in (b), i.e., 97 nm away from the substrate. (d) Polar plotting of the emission pattern in (b).

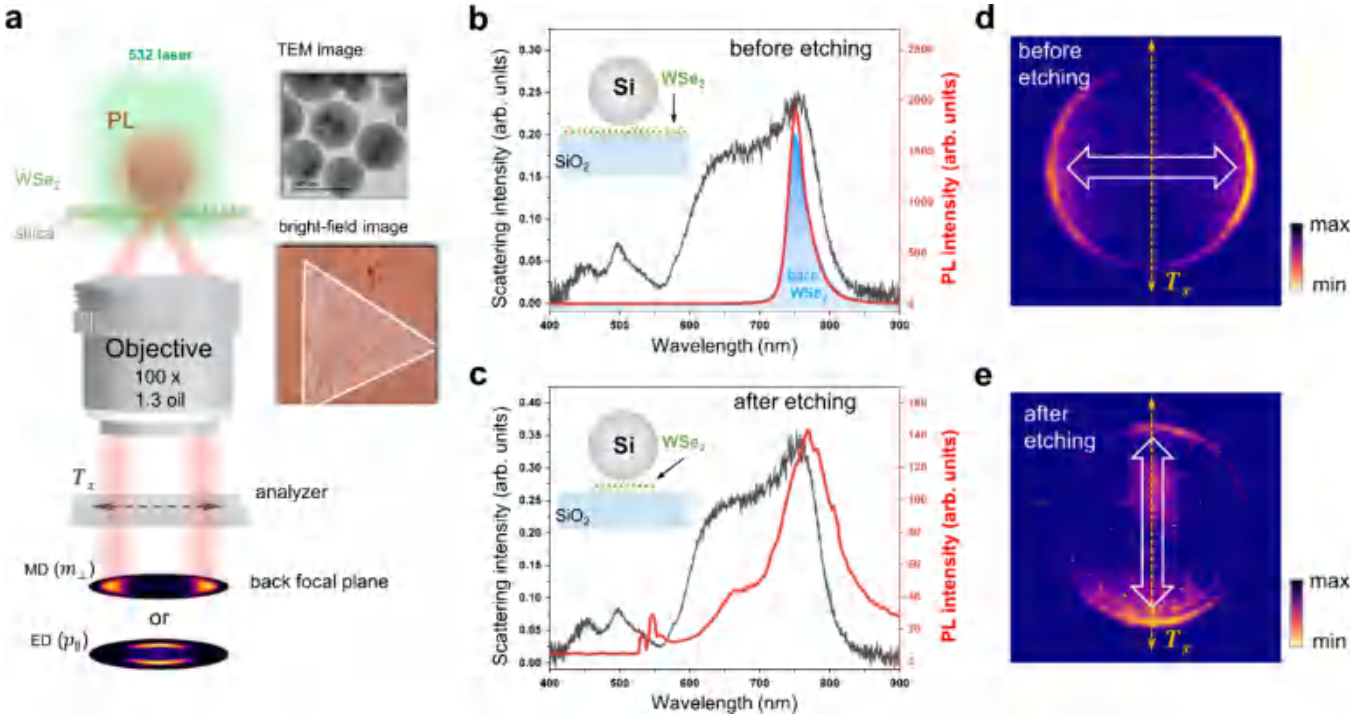

Figure 4. Measurement of the emission patterns of Si nanoparticles on a WSe_2 monolayer (SiNS/WSe_2). (a) Schematic illustration of the sample structure and the experimental setup for back focal imaging. T_x indicates the transmission axis of the analyzer. $m_\perp$ ($p_\parallel$) denotes the magnetic (electric) dipole source with a dipole moment orthogonal (parallel) to T_x. The analyzer let pass only the emission from $m_\perp$or $p_\parallel$. (b, c) Scattering and photoluminescence (PL) spectra measured for a SiNS/WSe_2 structure before (b) and after (c) plasma etching treatment. The PL spectrum of a bare WSe_2 monolayer was provided for reference (the blue curve). (d, e) Comparison of the back focal images of the SiNS/WSe_2 structure before (d) and after (e) etching. The spectral window for imaging is 550−900 nm. The exposure times for the BFI measurements in d and e are 0.1 and 0.5s, respectively.

their emission patterns inside the substrate.[44] Figure 3a shows the simulated emission pattern of a silica-supported ED emitter. As can be seen, most of the emission enters the substrate while exhibiting a two-lobes-shaped spatial profile. It should be noted that the orientation of the two emission lobes, along which the two lobes are aligned in the far-field projection plane (lower inset in Figure 3a), is orthogonal to the dipole moment of the ED source (p_x). At the presence of the SiNS, we observed a similar two-lobe-shaped emission pattern (Figure 3b) as the bare ED source on silica, but the two-

https://doi.org/10.1021/acs.nanolett.4c03760
Nano Lett. 2024, 24, 13315−13323

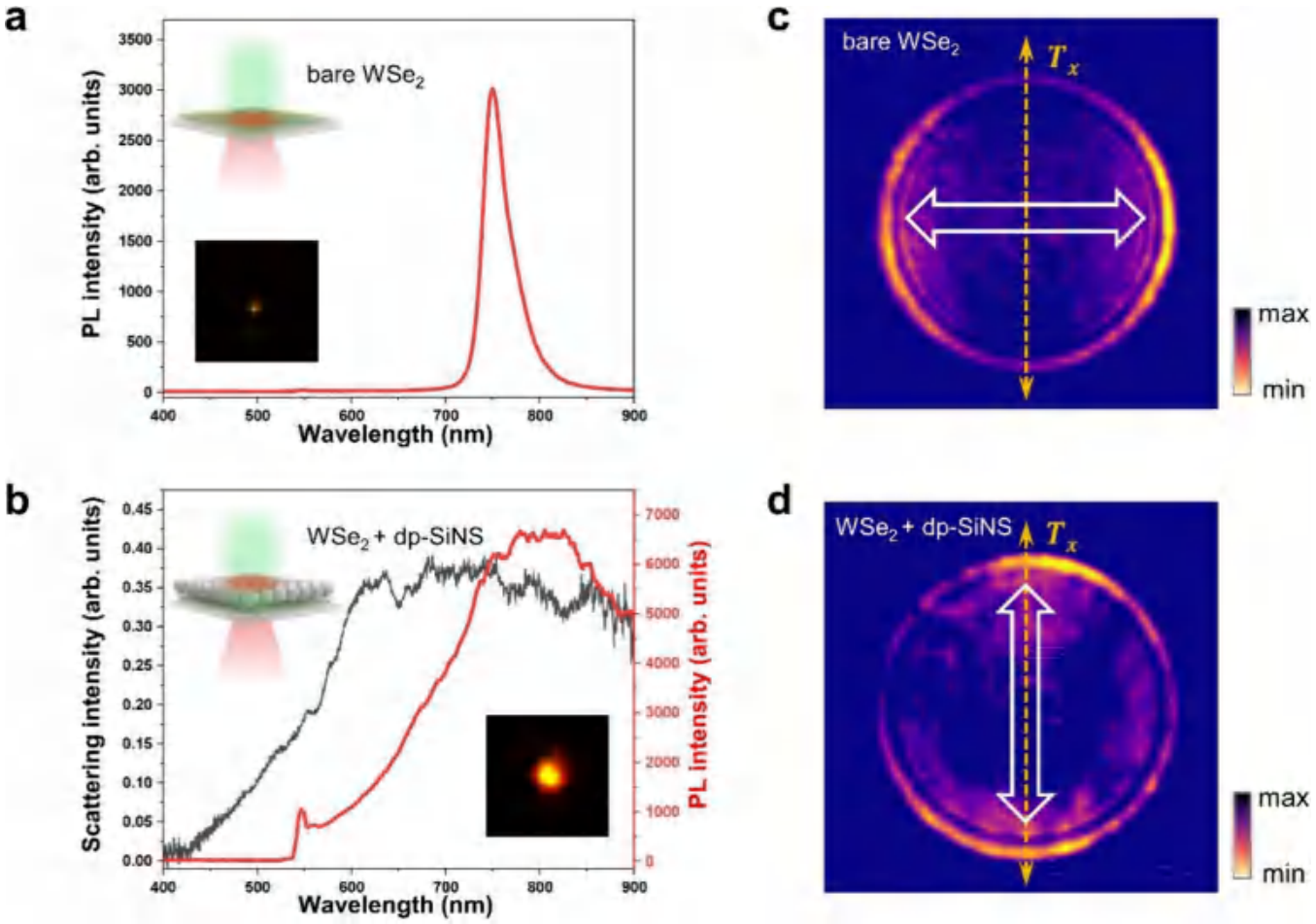

Figure 5. MD emission from WSe_2 coupled to a monolayer of densely packed Si nanoparticles (dp-SiNS). (a, b) Emission spectra of a bare WSe_2 monolayer (a) and that couples to dp-SiNS (b). Insets show the real-space photoluminescence images of the emission spots. (c, d) Back focal images of the structures shown in (a) and (b), respectively. T_x marks the transmission axis orientation of the analyzer, indicating the orientation of the electric dipole moment. The same exposure time of 0.1s was used for the BFI measurements in parts (c) and (d).

lobe orientation is no longer orthogonal to the dipole moment of the local ED source. Instead, it is rotated by a degree of 90°. The observation is in line with our anticipation that the coupling of the ED source to the SiNS transforms the ED emission to an MD type, which results in an MD-like source with a dipole moment rotated by 90° with respect to the original ED source (hereafter termed as m_y'). This can be further corroborated by comprising the emission patterns of this MD source (m_y') and a pure silica-supported MD source with the same dipole orientation (m_y) and a substrate-emitter separation equal to the radius of the SiNS. As displayed in Figure 3b and c, the m_y' and m_y sources show the same emission profiles, suggesting the substrated EDcSiNS functionally equals a pure MD light source.

Following the above analysis, the key to the fabrication of the EDcSiNS-based MD light sources is the availability of ED emitters having dipole moments tangential to the particle surface. Here we chose monolayered WSe_2 as the ED emitters, which features highly efficient photoluminescence emission originated from its excitonic-type ED transitions. The in-plane ED transitions of monolayered WSe_2 is about 2 orders of magnitude stronger than its out-of-plane counterpart,[45,46] thus offering the ideal candidate of an in-plane ED source for realization of the EDcSiNS architecture. Highly monodisperse Si nanospheres with a diameter of ∼180 nm was fabricated with the method in refs 47, 48 and then transferred to monolayered WSe_2 microflakes on a 0.17 mm-thick silica slide, forming the desired EDcSiNS nanoconstruct (see Figure 4a). They exhibit MD resonances around the exciton wavelength (∼750 nm) of the WSe_2 monolayer, which ensures resonance coupling between the MD antenna modes and the in-plane excitons. We would like to emphasis that the similar coupling structures comprising of silicon nanoparticles and a transition metal dichalcogenides (TMDC) monolayer (WS_2, MoS_2, etc.) had been investigated in quite a few studies,[25,49−52] but the associated emission characters and mode origins remain unexplored.

Next, a back-focal-plane (BFP) imaging setup was constructed to inspect the emission patterns of single EDcSiNS structures, as shown in Figure 4a (for more details see Methods and Figure S6). The sample was excited by a 532 nm-wavelenth laser, with the excited photoluminescence collected by an oil-immersed objective. An analyzer was inserted in the detection path to let through PL from an ED-type source with electric dipole moment parallel to the transmission axis (T_x), thereafter termed $p_{\parallel}$, or a MD-type source with magnetic dipole moment orthogonal to the transmission axis ($m_{\perp}$). Figure 4b shows the photoluminescence spectrum of a typical EDcSiNS structure. We can see that the emission of the single EDcSiNS exhibits spectral characters similar to those of a bare

https://doi.org/10.1021/acs.nanolett.4c03760
Nano Lett. 2024, 24, 13315−13323

WSe_2 monolayer. Besides, the emission peak overlaps well with the scattering MD resonance of the constituent Si nanoparticles, suggesting potential resonance coupling between the Si nanoparticles and the underlying WSe_2 monolayer. However, the BFP image of this EDcSiNS structure shows a two-lobe-shaped emission pattern oriented orthogonal to the transmission axis, a characteristic indicative of a $p_{\parallel}$-type emission source. This is reasonable considering the very small geometric cross-section of the nanoparticle (diameter ∼180 nm) with respect to the whole laser illumination area (a diffraction-limited spot size of ∼500 nm on the focal plane); the emission from the uncoupled WSe_2 background could dominate the total photoluminescence signal. To remove such uncoupled emission and solely resolve the emission from the nanoparticle coupled WSe_2, the sample is etched using a low-energy argon plasma where the silicon nanoparticle itself acts as an etching mask (see inset in Figure 4c).[46,52]

We did not observe marked modification of the scattering resonances of individual EDcSiNS structures by the etching treatment, as shown in Figure 4c. However, the measured photoluminescence spectrum exhibits a broader peak line width at around the scattering MD resonance wavelength of the EDcSiNS, implying the MD-modified WSe_2 emission via coupling to a Si nanoparticle. Particularly, the etched EDcSiNS exhibits a two-lobes-shaped emission pattern (Figure 4e), and the orientation of the two-lobes is rotated by 90° with respect to its unetched counterpart (Figure 4d) and bare WSe_2 monolayers (Figure 5a). These observations agree well with the theoretical results shown in Figure 3, unambiguously confirming the MD-type emission origin of the silicon nanoparticle coupled WSe_2 monolayer. Similar observations have also been made over other EDcSiNS with different particle sizes, despite the mismatching between the particle MD resonances and the excitonic wavelength of WSe_2 monolayers (see Figure S7).

Beyond the single EDcSiNS structures, we also resolved the MD emission characteristics of WSe_2 monolayers coupled to a monolayer of densely packed Si nanoparticles (dp-SiNS). As shown in Figure 5d, the two-lobe-shaped emission pattern of the WSe_2 monolayer rotates by 90° when it couples to the dp-SiNS, manifesting the transition of an ED-type emission origin (p_x) to a MD one (m_y). We emphasize that the MD emission features of the dp-SiNS coupled WSe_2 shown in Figure 5d can be directly resolved, with no need for the plasma etching treatment as that for the single EDcSiNS (Figure 4e). It should be noted that the inhomogeneity in the size of densely packed nanoparticles would result in varied MD resonance wavelengths, which overlap with each other and lead to the broad spectral response shown in Figure 5b. Besides, we resolved an ∼6× enhancement of the monolayered WSe_2 emission by coupling to the dp-SiNS (see insets in Figure 5a, b), which can be attributed to the MD resonance mediated Purcell effect.[22]

In summary, we have proposed the design of ideal magnetic dipole sources with silicon nanoparticle-coupled electric dipole emitters. For these hybrid structures, the constituent ED emitters are required to have dipole moments tangential to the particle surface and excite exclusively the MD resonance of the nanoparticle, through which the local emission is dressed with strong MD mode characters. As a proof of concept, we have realized such a MD source with a WSe_2 monolayer coupled Si nanoparticles and experimentally demonstrated ideal magnetic dipole emission in the visible spectral range. We anticipate that this mechanism can be generalized and applied to other magnetic nanoantenna-emitter nanosystems with elegant coupling configurations. For example, the coupling configuration demonstrated here can be extended to an optimized version consisting of a silicon nanoparticle coated with monolayered transition metal dichalcogenides,[53] which should support more efficient mode coupling interactions and thus enable further enhanced magnetic light emission. The potential applications of such efficient magnetic light sources include active Huygens metasurfaces and optical phase radars, for which the ideal magnetic light sources coherently interfering with their electric counterparts lead to perfect forward emission or even free beam directivity in full space.

METHODS

Sample Fabrication. Monolayered WSe_2 microflakes were synthesized using the chemical vapor deposition method and subsequently transferred onto a 0.17 mm thick silica slide. Highly monodisperse silicon nanospheres with crystalline quality were fabricated with a recently developed bottom-up approach that combines sequential annealing and etching treatments of commercial SiO lumps.[47,48] These colloidal nanoparticles were then drop-cast onto the WSe_2 microflakes and left dry in air.

Experimental Setup. The scattering responses of individual Si nanospheres were measured by using a commercial optical microscope (BX51, Olympus) equipped with a standard dark-field illumination module. A 50× dark-field objective (NA 0.8, MPLFLN, Olympus) was employed to collect the scattered light of a single Si nanosphere, which was subsequently directed either to a monochromator (SR500, Andor) equipped with a cooled CCD camera (DU970N, Andor) for spectral analysis or to a color CCD camera (Retiga R6, Teledyne Photometrics) for imaging.

The photoluminescence (PL) spectroscopy of silicon nanoparticles on a WSe_2 monolayer was performed by using an inverted microscope (Observer Z1, Zeiss). An oil-immersed objective (EC Plan-Neofluar, Zeiss) with a numerical aperture of 1.3 was employed to focus incident 532 nm-wavelengh laser (EXLSR-532−55−194, Spectra-Physis) onto the sample and collect the emitted photoluminescence signal. The PL was then delivered to a fiber-based spectrometer (QE Pro High-Performance, Ocean Insight) for spectral analysis or to a back-focal-plane imaging module to resolve the angular emission profile (for more details, see the Supporting Information).

Numerical Simulations. The electromagnetic numerical simulations throughout the main text were implemented by using the commercial finite-element solver (COMSOL Multiphysics) in the frequency domain. The dielectric constant of silicon was interpolated from the Palik experimental data.[54] A single Si nanosphere was illuminated either with a plane wave to resolve its Mie-type multipole resonances or by excited by a nearby electric dipole source to simulate the nanoparticle-modified emission responses. The multipole expansion of the emission from a single electric dipole emitter near a silicon nanosphere was implemented following the method in ref 24.

ASSOCIATED CONTENT

Supporting Information

The Supporting Information is available free of charge at https://pubs.acs.org/doi/10.1021/acs.nanolett.4c03760.

https://doi.org/10.1021/acs.nanolett.4c03760
Nano Lett. 2024, 24, 13315−13323

Extended simulation results show how the magnetic resonances of silicon nanoparticles are excited by local dipole emitters, the particle-emitter distance dependent emission characters, and the effect of a silica substrate on the scattering and emission spectra; derivation of the analytical model describing the emission response of an electric dipole near a silicon nanosphere; experimental setup; extended experimental study on the emission response of monolayered WSe_2 off-resonantly coupled to a silicon nanoparticle (PDF)

AUTHOR INFORMATION

Corresponding Author

Guang-Can Li − *Guangdong Provincial Key Laboratory of Nanophotonic Functional Materials and Devices, Guangdong Basic Research Center of Excellence for Structure and Fundamental Interactions of Matter, School of Optoelectronic Science and Engineering, South China Normal University, 510006 Guangzhou, China;* orcid.org/0000-0002-9903-8900; Email: Guangcan.li@m.scnu.edu.cn

Authors

Ruizhao Yao − *Guangdong Provincial Key Laboratory of Nanophotonic Functional Materials and Devices, Guangdong Basic Research Center of Excellence for Structure and Fundamental Interactions of Matter, School of Optoelectronic Science and Engineering, South China Normal University, 510006 Guangzhou, China;* orcid.org/0009-0008-2967-550X

Hiroshi Sugimoto − *Department of Electrical and Electronic Engineering, Graduate School of Engineering, Kobe University, Kobe 657-8501, Japan;* orcid.org/0000-0002-1520-0940

Tianhua Feng − *Department of Electronic Engineering, College of Information Science and Technology, Jinan University, Guangzhou 510632, China;* orcid.org/0000-0002-7271-2512

Minoru Fujii − *Department of Electrical and Electronic Engineering, Graduate School of Engineering, Kobe University, Kobe 657-8501, Japan*

Shimei Liu − *Guangdong Provincial Key Laboratory of Nanophotonic Functional Materials and Devices, Guangdong Basic Research Center of Excellence for Structure and Fundamental Interactions of Matter, School of Optoelectronic Science and Engineering, South China Normal University, 510006 Guangzhou, China;* orcid.org/0000-0001-5704-095X

Xinming Li − *Guangdong Provincial Key Laboratory of Nanophotonic Functional Materials and Devices, Guangdong Basic Research Center of Excellence for Structure and Fundamental Interactions of Matter, School of Optoelectronic Science and Engineering, South China Normal University, 510006 Guangzhou, China*

Sheng Lan − *Guangdong Provincial Key Laboratory of Nanophotonic Functional Materials and Devices, Guangdong Basic Research Center of Excellence for Structure and Fundamental Interactions of Matter, School of Optoelectronic Science and Engineering, South China Normal University, 510006 Guangzhou, China;* orcid.org/0000-0002-7277-0042

Complete contact information is available at: https://pubs.acs.org/10.1021/acs.nanolett.4c03760

Author Contributions

G. C. Li conceived the idea and supervised the project. R. Z. Yao set up the experimental rigs, performed all the experimental measurements and electromagnetic numerical simulations. T. H. Feng developed the analytical model. H. Sugimoto, M. Fujii, S. M Liu, X. M. Li and S. Lan helped with sample preparation and corresponding characterizations. G. C. Li wrote and finalized the manuscript with input from all the authors.

Notes

The authors declare no competing financial interest.

ACKNOWLEDGMENTS

This work was financially supported by the National Natural Science Foundation of China (Grant No. 12274147 and U23A20369), The Natural Science Foundation of Guangdong Province (Grant No. 2023A1515012368), the Natural Science Foundation of Guangzhou (Grant No. 202201010445) and the International Academic Exchange Program of Guangdong Province (Grant No. 2022A0505030012). This work was partially supported by JSPS KAKENHI, Grant Number 22K18949, and JST FOREST Program, Grant Number JPMJFR213L, and Kobe University Strategic International Collaborative Research Grant. We thank Prof. Yongliang Zhang (Institute of Semiconductors, CAS) for the useful discussion.

REFERENCES

(1) Alu, A.; Shalaev, V.; Loncar, M.; Sorger, V. J. Metasurfaces-from Science to Applications. *Nanophotonics* **2018**, *7* (6), 949−951.

(2) Lu, W.; Menezes, L. D. S.; Tittl, A.; Ren, H.; Maier, S. A. Active Huygens' Metasurface Based on in-Situ Grown Conductive Polymer. *Nanophotonics* **2024**, *13* (1), 39−49.

(3) Daqiqeh Rezaei, S.; Dong, Z.; You En Chan, J.; Trisno, J.; Ng, R. J. H.; Ruan, Q.; Qiu, C. W.; Mortensen, N. A.; Yang, J. K. W. Nanophotonic Structural Colors. *ACS Photonics* **2021**, *8* (1), 18−33.

(4) Badloe, T.; Kim, J.; Kim, I.; Kim, W. S.; Kim, W. S.; Kim, Y. K.; Rho, J. Liquid Crystal-Powered Mie Resonators for Electrically Tunable Photorealistic Color Gradients and Dark Blacks. *Light Sci. Appl.* **2022**, *11* (1), 118.

(5) Vermeulen, D.; Cole, D. B.; Raval, M.; Poulton, C. V.; Watts, M. R.; Byrd, M. J.; Yaacobi, A. Coherent Solid-State LIDAR with Silicon Photonic Optical Phased Arrays. *Opt. Lett.* **2017**, *42* (20), 4091−4094.

(6) Hsu, C. P.; Li, B.; Solano-Rivas, B.; Gohil, A. R.; Chan, P. H.; Moore, A. D.; Donzella, V. A Review and Perspective on Optical Phased Array for Automotive LiDAR. *IEEE J. Sel. Top. Quantum Electron* **2021**, *27* (1), 1−16.

(7) Ofelt, G. S. Intensities of Crystal Spectra of Rare-Earth Ions. *J. Chem. Phys.* **1962**, *37* (3), 511−520.

(8) Judd, B. R. Optical Absorption Intensities of Rare-Earth Ions. *Phys. Rev.* **1962**, *127* (3), 750.

(9) Carnall, W. T.; Fields, P. R.; Rajnak, K. Spectral Intensities of the Trivalent Lanthanides and Actinides in Solution. II. Pm3+, Sm3+, Eu3+, Gd3+, Tb3+, Dy3+, and Ho3+. *J. Chem. Phys.* **1968**, *49* (10), 4412−4423.

(10) Zurita-Sánchez, J. R.; Novotny, L. Multipolar Interband Absorption in a Semiconductor Quantum Dot I Electric Quadrupole Enhancement. *J. Opt. Soc. Am. B* **2002**, *19* (6), 1355−1362.

(11) Li, D.; Karaveli, S.; Cueff, S.; Li, W.; Zia, R. Probing the Combined Electromagnetic Local Density of Optical States with Quantum Emitters Supporting Strong Electric and Magnetic Transitions. *Phys. Rev. Lett.* **2018**, *121* (22), 227403.

(12) Brewer, N. R.; Buckholtz, Z. N.; Simmons, Z. J.; Mueller, E. A.; Yavuz, D. D. Coherent Magnetic Response at Optical Frequencies Using Atomic Transitions. *Phys. Rev. X* **2017**, *7* (1), No. 011005.

(13) Weber, M. J. Radiative and Multiphonon Relaxation of Rare-Earth Ions in Y2O3. *Phys. Rev.* **1968**, *171* (2), 283.
(14) Monticone, F.; Alù, A. The Quest for Optical Magnetism: From Split-Ring Resonators to Plasmonic Nanoparticles and Nanoclusters. *J. Mater. Chem. C* **2014**, *2* (43), 9059−9072.
(15) Smith, D. R.; Pendry, J. B.; Wiltshire, M. C. K. Metamaterials and Negative Refractive Index. *Science* **2004**, *305* (5685), 788−792.
(16) Yen, T. J.; Padilla, W. J.; Fang, N.; Vier, D. C.; Smith, D. R.; Pendry, J. B.; Basov, D. N.; Zhang, X. Terahertz Magnetic Response from Artificial Materials. *Science* **2004**, *303* (5663), 1494−1496.
(17) Meng, Y.; Zhang, Q.; Lei, D.; Li, Y.; Li, S.; Liu, Z.; Xie, W.; Leung, C. W. Plasmon-Induced Optical Magnetism in an Ultrathin Metal Nanosphere-Based Dimer-on-Film Nanocavity. *Laser Photonics Rev.* **2020**, *14* (9), 2000068.
(18) Fan, J. A.; Wu, C.; Bao, K.; Bao, J.; Bardhan, R.; Halas, N. J.; Manoharan, V. N.; Nordlander, P.; Shvets, G.; Capasso, F. Self-Assembled Plasmonic Nanoparticle Clusters. *Science* **2010**, *328* (5982), 1135−1138.
(19) Shafiei, F.; Monticone, F.; Le, K. Q.; Liu, X. X.; Hartsfield, T.; Alù, A.; Li, X. A Subwavelength Plasmonic Metamolecule Exhibiting Magnetic-Based Optical Fano Resonance. *Nat. Nanotechnol.* **2013**, *8* (2), 95−99.
(20) Kuznetsov, A. I.; Miroshnichenko, A. E.; Brongersma, M. L.; Kivshar, Y. S.; Luk'yanchuk, B. Optically Resonant Dielectric Nanostructures. *Science* **2016**, *354* (6314), 2472.
(21) Jahani, S.; Jacob, Z. All-Dielectric Metamaterials. *Nat. Nanotechnol.* **2016**, *11* (1), 23−36.
(22) Baranov, D. G.; Savelev, R. S.; Li, S. V.; Krasnok, A. E.; Alù, A. Modifying Magnetic Dipole Spontaneous Emission with Nanophotonic Structures. *Laser Photonics Rev.* **2017**, *11* (3), 1600268.
(23) Liu, Y.; Lau, S. C.; Cheng, W. H.; Johnson, A.; Li, Q.; Simmerman, E.; Karni, O.; Hu, J.; Liu, F.; Brongersma, M. L.; Heinz, T. F.; Dionne, J. A. Controlling Valley-Specific Light Emission from Monolayer MoS2 with Achiral Dielectric Metasurfaces. *Nano Lett.* **2023**, *23* (13), 6124−6131.
(24) Qin, F.; Zhang, Z.; Zheng, K.; Xu, Y.; Fu, S.; Wang, Y.; Qin, Y. Transverse Kerker Effect for Dipole Sources. *Phys. Rev. Lett.* **2022**, *128* (19), 193901.
(25) Shinomiya, H.; Sugimoto, H.; Hinamoto, T.; Lee, Y. J.; Brongersma, M. L.; Fujii, M. Enhanced Light Emission from Monolayer MoS2 by Doubly Resonant Spherical Si Nanoantennas. *ACS Photonics* **2022**, *9* (5), 1741−1747.
(26) Mignuzzi, S.; Vezzoli, S.; Horsley, S. A. R.; Barnes, W. L.; Maier, S. A.; Sapienza, R. Nanoscale Design of the Local Density of Optical States. *Nano Lett.* **2019**, *19* (3), 1613−1617.
(27) Ernandes, C.; Lin, H. J.; Mortier, M.; Gredin, P.; Mivelle, M.; Aigouy, L. Exploring the Magnetic and Electric Side of Light through Plasmonic Nanocavities. *Nano Lett.* **2018**, *18* (8), 5098−5103.
(28) Zhang, Y.; Yue, P.; Liu, J.-Y.; Geng, W.; Bai, Y.-T.; Liu, S.-D. Ideal Magnetic Dipole Resonances with Metal-Dielectric-Metal Hybridized Nanodisks. *Opt. Express* **2019**, *27* (11), 16143−16155.
(29) Mivelle, M.; Grosjean, T.; Burr, G. W.; Fischer, U. C.; Garcia-Parajo, M. F. Strong Modification of Magnetic Dipole Emission through Diabolo Nanoantennas. *ACS Photonics* **2015**, *2* (8), 1071−1076.
(30) Chigrin, D. N.; Kumar, D.; Cuma, D.; Von Plessen, G. Emission Quenching of Magnetic Dipole Transitions near a Metal Nanoparticle. *ACS Photonics* **2016**, *3* (1), 27−34.
(31) Khurgin, J. B. How to Deal with the Loss in Plasmonics and Metamaterials. *Nat. Nanotechnol.* **2015**, *10* (1), 2−6.
(32) Staude, I.; Pertsch, T.; Kivshar, Y. S. All-Dielectric Resonant Meta-Optics Lightens Up. *ACS Photonics* **2019**, *6* (4), 802−814.
(33) Li, G. C.; Xiang, J.; Zhang, Y. L.; Deng, F.; Panmai, M.; Zhuang, W.; Lan, S.; Lei, D. Mapping the Magnetic Field Intensity of Light with the Nonlinear Optical Emission of a Silicon Nanoparticle. *Nano Lett.* **2021**, *21* (6), 2453−2460.
(34) Zhang, C.; Xu, Y.; Liu, J.; Li, J.; Xiang, J.; Li, H.; Li, J.; Dai, Q.; Lan, S.; Miroshnichenko, A. E. Lighting up Silicon Nanoparticles with Mie Resonances. *Nat. Commun.* **2018**, *9* (1), 2964.
(35) Matsumori, A.; Sugimoto, H.; Fujii, M. Silicon Nanosphere with Accessible Magnetic Hotspot. *Adv. Opt. Mater.* **2022**, *10* (8), 2102574.
(36) Li, J.; Verellen, N.; Van Dorpe, P. Enhancing Magnetic Dipole Emission by a Nano-Doughnut-Shaped Silicon Disk. *ACS Photonics* **2017**, *4* (8), 1893−1898.
(37) Feng, T.; Zhang, W.; Liang, Z.; Xu, Y.; Miroshnichenko, A. E. Isotropic Magnetic Purcell Effect. *ACS Photonics* **2018**, *5* (3), 678−683.
(38) Feng, T.; Xu, Y.; Liang, Z.; Zhang, W. All-Dielectric Hollow Nanodisk for Tailoring Magnetic Dipole Emission. *Opt. Lett.* **2016**, *41* (21), 5011−5014.
(39) Yang, Y.; Zhu, B.; Dai, H.; Sun, X. Identical Emission Enhancement for Arbitrary-Orientation Magnetic Dipole Emitters in Silicon Hollow Nanocavity. *Opt. Express* **2019**, *27* (18), 25931−25942.
(40) Vaskin, A.; Mashhadi, S.; Steinert, M.; Chong, K. E.; Keene, D.; Nanz, S.; Abass, A.; Rusak, E.; Choi, D. Y.; Fernandez-Corbaton, I.; Pertsch, T.; Rockstuhl, C.; Noginov, M. A.; Kivshar, Y. S.; Neshev, D. N.; Noginova, N.; Staude, I. Manipulation of Magnetic Dipole Emission from Eu 3+ with Mie-Resonant Dielectric Metasurfaces. *Nano Lett.* **2019**, *19* (2), 1015−1022.
(41) Sanz-Paz, M.; Ernandes, C.; Esparza, J. U.; Burr, G. W.; Van Hulst, N. F.; Maitre, A.; Aigouy, L.; Gacoin, T.; Bonod, N.; Garcia-Parajo, M. F.; Bidault, S.; Mivelle, M. Enhancing Magnetic Light Emission with All-Dielectric Optical Nanoantennas. *Nano Lett.* **2018**, *18* (6), 3481−3487.
(42) Sugimoto, H.; Fujii, M. Magnetic Purcell Enhancement by Magnetic Quadrupole Resonance of Dielectric Nanosphere Antenna. *ACS Photonics* **2021**, *8* (6), 1794−1800.
(43) Yao, K.; Zheng, Y. Directional Light Emission by Electric and Magnetic Dipoles near a Nanosphere: An Analytical Approach Based on the Generalized Mie Theory. *Opt. Lett.* **2021**, *46* (2), 302.
(44) Taminiau, T. H.; Karaveli, S.; Van Hulst, N. F.; Zia, R. Quantifying the Magnetic Nature of Light Emission. *Nat. Commun.* **2012**, *3* (1), 979.
(45) Mueller, N. S.; Arul, R.; Kang, G.; Saunders, A. P.; Johnson, A. C.; Sánchez-Iglesias, A.; Hu, S.; Jakob, L. A.; Bar-David, J.; de Nijs, B.; Liz-Marzán, L. M.; Liu, F.; Baumberg, J. J. Photoluminescence Upconversion in Monolayer WSe2 Activated by Plasmonic Cavities through Resonant Excitation of Dark Excitons. *Nat. Commun.* **2023**, *14* (1), 5726.
(46) Lo, T. W.; Chen, X.; Zhang, Z.; Zhang, Q.; Leung, C. W.; Zayats, A. V.; Lei, D. Plasmonic Nanocavity Induced Coupling and Boost of Dark Excitons in Monolayer WSe2 at Room Temperature. *Nano Lett.* **2022**, *22* (5), 1915−1921.
(47) Sugimoto, H.; Okazaki, T.; Fujii, M. Mie Resonator Color Inks of Monodispersed and Perfectly Spherical Crystalline Silicon Nanoparticles. *Adv. Opt. Mater.* **2020**, *8* (12), 2000033.
(48) Hinamoto, T.; Hotta, S.; Sugimoto, H.; Fujii, M. Colloidal Solutions of Silicon Nanospheres toward All-Dielectric Optical Metafluids. *Nano Lett.* **2020**, *20* (10), 7737−7743.
(49) Liu, S.-D.; Fan, J.-L.; Wang, W.-J.; Chen, J.-D.; Chen, Z.-H. Resonance Coupling between Molecular Excitons and Nonradiating Anapole Modes in Silicon Nanodisk-J-Aggregate Heterostructures. *ACS Photonics* **2018**, *5* (4), 1628−1639.
(50) Fang, J.; Yao, K.; Wang, M.; Yu, Z.; Zhang, T.; Jiang, T.; Huang, S.; Korgel, B. A.; Terrones, M.; Alù, A.; Zheng, Y. Observation of Room-Temperature Exciton-Polariton Emission from Wide-Ranging 2D Semiconductors Coupled with a Broadband Mie Resonator. *Nano Lett.* **2023**, *23* (21), 9803−9810.
(51) Fang, J.; Yao, K.; Zhang, T.; Wang, M.; Jiang, T.; Huang, S.; Korgel, B. A.; Terrones, M.; Alù, A.; Zheng, Y. Room-Temperature Observation of Near-Intrinsic Exciton Linewidth in Monolayer WS2. *Adv. Mater.* **2022**, *34* (15), 2108721.
(52) Cihan, A. F.; Curto, A. G.; Raza, S.; Kik, P. G.; Brongersma, M. L. Silicon Mie Resonators for Highly Directional Light Emission from Monolayer MoS2. *Nat. Photonics* **2018**, *12* (5), 284−290.

https://doi.org/10.1021/acs.nanolett.4c03760
Nano Lett. 2024, 24, 13315−13323

(53) Hinamoto, T.; Lee, Y. S.; Dereshgi, S. A.; DiStefano, J. G.; dos Reis, R.; Sugimoto, H.; Aydin, K.; Fujii, M.; Dravid, V. P. Resonance Couplings in Si@MoS2 Core−Shell Architectures. *Small* **2022**, *18* (17), No. 2200413.
(54) Palik, E. D. *Handbook of Optical Constants of Solids*; Elsevier, 1985; Vol. *1*.

https://doi.org/10.1021/acs.nanolett.4c03760
Nano Lett. 2024, 24, 13315−13323